# Double-Concave Binding of Bicorannulenyl Dianion: Cesium vs Lithium Salts

**ARTICLE** *in* ORGANOMETALLICS · JUNE 2014

Impact Factor: 4.13 · DOI: 10.1021/om500396m

ORGANOMETALLICS

Article

pubs.acs.org/Organometallics

# Double-Concave Binding of Bicorannulenyl Dianion: Cesium vs Lithium Salts

Natalie J. Sumner,[†] Sarah N. Spisak,[†] Alexander S. Filatov,[†] Andrey Yu. Rogachev,[‡] Alexander V. Zabula,[§] and Marina A. Petrukhina*[,†]

[†]Department of Chemistry, University at Albany, State University of New York, Albany, New York 12222, United States

[‡]Department of Biological and Chemical Sciences, Illinois Institute of Technology, Chicago, Illinois 60616, United States

[§]Department of Chemistry, University of Wisconsin, Madison, Wisconsin 53706, United States

Supporting Information

**ABSTRACT:** The first X-ray structural characterization of bicorannulenyl dianion has been accomplished for two alkali metal salts, $[Li^+(THF)_4]_2[C_{40}H_{18}^{2-}]$ (**1**) and $[Cs^+(18\text{-crown-6})]_2[C_{40}H_{18}^{2-}]$ (**2**). This crystallographic study revealed the biaryl stereochemistry, geometry transformation upon acquiring two electrons, and different binding preferences of $Li^+$ vs $Cs^+$ ions in the solid-state products.

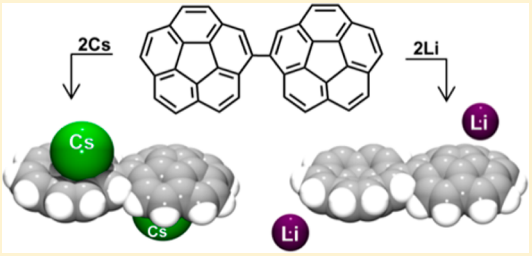


The design and synthesis of extended $\pi$-systems utilizing bowl-shaped polyarenes as functional building units has become a new research direction in recent years.[1,2] Varying the length and nature of the linkage between the curved fragments is effectively used to alter the electronic coupling and supramolecular oligomerization behavior, giving rise to new properties and interesting applications of the resulting carbon-rich compounds. The small bowl-shaped polyarene corannulene ($C_{20}H_{10}$) is commonly used for such applications due to its availability based on the well-developed preparation methods.[3] Using corannulene pincers, remarkable molecular receptors have been prepared with unique molecular recognition toward fullerene binding based on complementary convex−concave $\pi-\pi$ stacking interactions.[4] Fusion of corannulene units to anion-responsive $\pi$-conjugated molecules afforded novel self-organized molecular materials with enhanced charge carrier mobility.[5] Self-assembly of $\pi$-bowls coupled with redox-active organometallic spacers in corannulenylferrocenes and sumaneylferrocenes has also been explored.[6]

Direct aryl−aryl coupling of two corannulene bowls affords bicorannulenyl ($C_{40}H_{18}$, Scheme 1), which exhibits a novel chirality and unique dynamic stereochemistry elucidated by Shenhar's group using variable-temperature NMR spectroscopy and DFT calculations.[7] Recently, such isomerism was also found by Hirao and co-workers for bisumanenyl, having two linked sumanene ($C_{21}H_{12}$) bowls.[8] The redox properties of such extended aromatic systems composed of coupled bowl-shaped fragments, known to be excellent individual reservoirs for multiple electrons,[9] are especially interesting.[10] The reduction of bicorannulenyl has been previously investigated using solution NMR spectroscopy augmented by DFT calculations.[11] The in-depth investigation of the stereodynamics of bicorannulenyl dianion revealed 13 stable conformations: six pairs of enantiomers and a single achiral isomer ($PM_{180}$). Such flexibility led to problems with unequivocal interpretation of NMR data for the *in situ* formed bicorannulenyl dianion. While there are three stable diastereomers that are more energetically favorable, the $PM_{180}$ isomer was proposed to be the major species existing in solution. On the basis of the bond-order considerations, it was also predicted that the single bond tethering two corannulene units in bicorannulenyl should gain substantial double-bond character upon acquisition of two electrons, converting it to a charged overcrowded ethylene (Scheme 1).[11] Until now, no solid-state products of charged bicorannulenyl have been reported to give further insights on the stereochemistry and geometry transformation of $C_{40}H_{18}$ upon acquiring extra electrons.

In this work, we targeted the isolation of crystalline products of bicorannulenyl dianion in order to perform its first crystallographic investigation and to evaluate its metal-binding properties. We selected lithium and cesium for this study, as these two alkali metals show distinctly different binding preferences toward corannulene anions. While lithium ions

**Scheme 1. Transformation of Bicorannulenyl upon Reduction to Dianion**

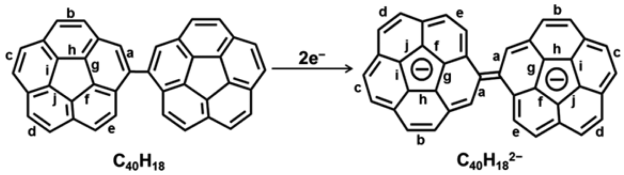


**Received:** April 14, 2014
**Published:** May 21, 2014

prefer to form solvent-separated ion pairs (SSIP) with corannulene mono- and dianion,[12] cesium exhibits unique concave binding in the contact ion pair (CIP) complex with the monoreduced bowl.[13] If the trend persists for the biaryl composed of two tethered corannulene units, the resulting products should provide us with an intersting pair for structural comparison: a "naked" dianion vs one having both bowls occupied by large cesium ions.

## RESULTS AND DISCUSSION

The reduction of $C_{40}H_{18}$ has been previously investigated using lithium[11b] and potassium[11a] metals as the reducing agents. The formation of the diamagnetic dianion has been observed by $^1$H NMR at low temperature as the first reduction step. Further reduction, monitored by $^1$H NMR spectroscopy, indicated the formation of bicorannulenyl tetraanion as the next distinctive product.[11a] The highest reduction state of $C_{40}H_{18}$, the octaanion, has been detected *in situ* using an excess of lithium metal. The interpretation of $^1$H NMR and $^7$Li NMR data suggested that these highly charged anions form supramolecular stacked aggregates with lithium ions in solution.[11b] The reduction of bicorannulenyl with the heavier metals of Group I has not yet been explored.

The controlled reduction of bicorannulenyl by lithium (2.5 equiv) in THF resulted in the formation of an intense purple solution characteristic of the dianion, $C_{40}H_{18}^{2-}$. However, the use of this method for the reduction of $C_{40}H_{18}$ with cesium metal was problematic due to very low product solubility. To resolve this issue, we found that addition of 18-crown-6 ether (2.1 equiv) to the THF solution of bicorannulenyl, prior to the addition of cesium metal, allowed the isolation of the target product (Scheme 2).

**Scheme 2. Preparation of Lithium and Cesium Salts of Bicorannulenyl Dianion**

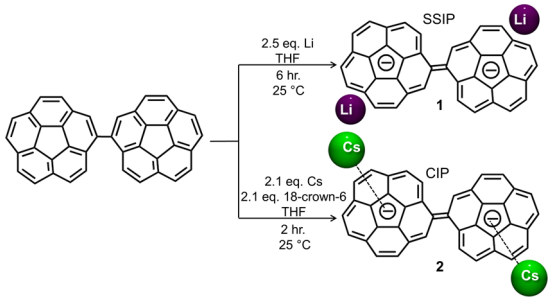


The single crystals of the resulting products, $[Li^+(THF)_4]_2[C_{40}H_{18}^{2-}]$ (**1**) and $[Cs^+(18\text{-crown-}6)]_2[C_{40}H_{18}^{2-}]$ (**2**), were isolated in good yield by layering the THF solutions with hexanes (with the addition of 18-crown-6 ether in the latter system). In the UV−vis spectra of crystals of **1** and **2** dissolved in THF (as well as for the *in situ* generated dianions, Figures S1 and S4), the maximum of the absorption band of the dianion in cesium salt (935 nm) is shifted compared to that in lithium salt (931 nm).

An X-ray diffraction study of $[Li^+(THF)_4]_2[C_{40}H_{18}^{2-}]$ (**1**) revealed the formation of a solvent-separated ion pair composed of the $C_{40}H_{18}^{2-}$ dianion and two $[Li^+(THF)_4]$ cations (Figure 1). In the cationic parts, the $Li^+$ ions are bound to four THF molecules with the Li···O bond distances (1.916(4)−1.959(4) Å) being similar to those observed previously.[12] In the solid state, both the convex and concave

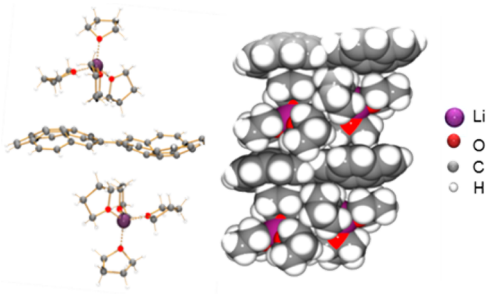


**Figure 1.** Molecular structure (left) and space-filling depiction of solid-state packing (right) of $[Li^+(THF)_4]_2[C_{40}H_{18}^{2-}]$.

faces of the dianion, $C_{40}H_{18}^{2-}$, are involved in weak intermolecular interactions with hydrogen atoms of the $[Li^+(THF)_4]$ moieties, with the shortest C−H···$\pi$ separations measured at 2.904 and 2.628 Å, respectively.

An X-ray diffraction study of $[Cs^+(18\text{-crown-}6)]_2[C_{40}H_{18}^{2-}]$ (**2**) revealed the formation of a contact ion pair between two $[Cs^+(18\text{-crown-}6)]$ cations and the $C_{40}H_{18}^{2-}$ anion. Each corannulene bowl of $C_{40}H_{18}^{2-}$ has an endo-bound $Cs^+$ ion capped with 18-crown-6 ether (Figure 2). Notably, concave

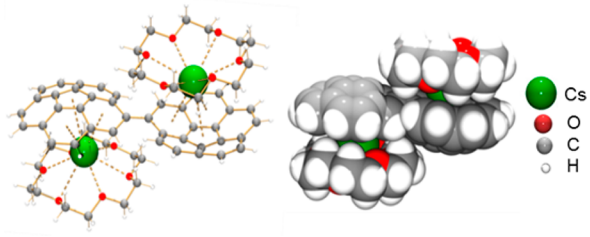


**Figure 2.** Molecular structure (left) and space-filling depiction (right) of $[Cs^+(18\text{-crown-}6)]_2[C_{40}H_{18}^{2-}]$.

metal binding to $\pi$-bowls is rare[14] and has been seen in several transition metal complexes of sumanene.[15] For corannulene, it was observed only in one cesium salt, $[Cs^+(18\text{-crown-}6)][C_{20}H_{10}^-]$.[13]

In contrast to the symmetrical $\eta^5$-endo hub coordination (Cs···C 3.424−3.573, Cs···$C_5$ centroid 3.285 Å) found in the aforementioned cesium salt with corannulene monoanion, the $Cs^+$ ions are shifted toward the central tether in **2** (Scheme 3).

**Scheme 3. Cesium Ion Binding in $[Cs^+(18\text{-crown-}6)][C_{20}H_{10}^-]$ (left) and 2 (right)**

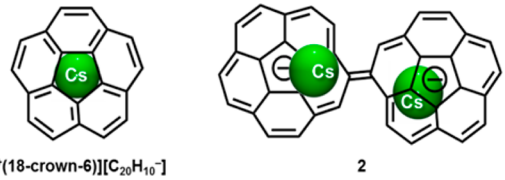


The shortest Cs···C contacts are observed with the two benzene rings adjacent to the double bond (Cs···$C_6$ centroid 3.304−3.425 Å) and with the central five-membered ring (Cs···$C_5$ centroid 3.474 Å). Additional Cs···C contacts with flank C atoms of the corannulene bowl are in the range 3.616−3.899 Å. Owing to its large size, the $Cs^+$ ion does not fit inside the 18-crown-6 ring and is pulled out toward the bicorannulenyl ligand. The Cs···O bond distances (3.048(4)−3.284(4) Å) are


dx.doi.org/10.1021/om500396m | *Organometallics* 2014, 33, 2874−2878

Table 1. Calculated and Experimental Values of Central Bond Length (Å), Angles (deg), and Rim and Hub Bond Lengths (Å) for $C_{40}H_{18}^{2-}$ vs $C_{40}H_{18}$ and $C_{20}H_{10}^{-}$

| | 1[a] | 1 | 2[a] | 2 | $C_{40}H_{18}$[7] | $C_{40}H_{18}^{2-}$[b] | $[C_{20}H_{10}^{-}]$[16] |
|---|---|---|---|---|---|---|---|
| | X-ray | calc | X-ray | calc | X-ray | calc | X-ray |
| central bond | 1.42(2) | 1.410 | 1.43(4) | 1.412 | 1.483(7) | 1.414 | |
| twist angle | 180 | 180 | 180 | 180 | 38 | 180 | |
| rim | | | | | | | |
| a | 1.479(15) | 1.468 | 1.481(17) | 1.469 | 1.381(9) | 1.464 | 1.412(3) |
| b | 1.380(13) | 1.379 | 1.377(13) | 1.381 | 1.344(10) | 1.380 | 1.382(3) |
| c | 1.401(15) | 1.408 | 1.421(16) | 1.407 | 1.345(10) | 1.412 | 1.391(3) |
| d | 1.357(15) | 1.386 | 1.362(15) | 1.386 | 1.339(9) | 1.387 | 1.403(3) |
| e | 1.420(14) | 1.420 | 1.397(15) | 1.409 | 1.354(8) | 1.407 | 1.392(3) |
| hub | | | | | | | |
| f | 1.420(7) | 1.419 | 1.424(10) | 1.422 | 1.456(9) | 1.421 | 1.422(2) |
| g | 1.411(7) | 1.402 | 1.403(10) | 1.420 | 1.451(10) | 1.418 | 1.402(2) |
| h | 1.399(7) | 1.420 | 1.406(10) | 1.402 | 1.475(10) | 1.398 | 1.410(2) |
| i | 1.416(7) | 1.405 | 1.421(11) | 1.420 | 1.466(10) | 1.426 | 1.4229(2) |
| j | 1.409(7) | 1.420 | 1.409(10) | 1.405 | 1.448(9) | 1.405 | 1.414(2) |
| bowl depth | 0.88 | 0.85 | 0.89 | 0.85 | 0.85 | 0.86 | 0.85 |

[a]Average values. [b]Free form.

close to those previously reported for $[Cs^+(18\text{-crown-}6)]$ salts with corannulene monoanion.[13]

The X-ray diffraction study of **1** and **2** revealed that only one isomer of $C_{40}H_{18}^{2-}$, the achiral $PM_{180}$ isomer, is present in the solid state (Table 1). As predicted earlier,[11] the central carbon−carbon bond between two corannulene units is shortened in **1** (1.42(2) Å) and **2** (1.43(4) (Å) in comparison with neutral bicorannulenyl (1.483(7) Å),[7] confirming a substantial double-bond character in both products. The latter is supported by DFT calculations that show almost no difference between the Li and Cs products (the calculated bond orders are 1.40 and 1.39, respectively). For comparison, the analogous bond order in the $C_{40}H_{18}^{2-}$ anion free of any interactions is equal to 1.39, as calculated at the same level of theory. Details of electronic structure of the bicorannylenyl dianion in different environments are discussed below.

It can be noted here that the $PM_{180}$ conformation should be favorable for the double-bond character of the tether, as it allows minimizing steric crowding around the central bond. The bond length distribution along the rim of the dianion consists of alternating double and single C−C bonds (Table 1). The hub bond length distribution is similar to that found in the monoanion of corannulene.[12,13,16] Notably, despite different metal-binding modes, there is no substantial difference in geometric parameters of $C_{40}H_{18}^{2-}$ in **1** and **2**. Additionally, the depth of each bowl in **1** and **2** is not significantly different from neutral bicorannulenyl or the corannulene monoanion.[7,12,13,16]

The asymmetric concave binding of $Cs^+$ ions to the endo surface of $C_{40}H_{18}^{2-}$ in **2** prompted us to look into the electronic structure and charge distribution of the dianion using theoretical methods. A molecular electrostatic potential map (MEP) is often used for the vizualization of the charge distribution over the polyaromatic surfaces.[17] In **2**, the electron density is not symmetrically distributed over the dianion surface and is shifted toward the central tether and the surrounding C atoms on the concave face (Figure 3). Since the interaction between $Cs^+$ and the $C_{40}H_{18}^{2-}$ anion is predominately electrostatic, this charge distribution leads to the shift of the metal-binding site away from the central hub ring, resulting in the observed cesium placement.

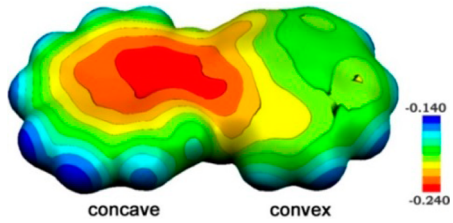


Figure 3. Molecular electrostatic potential map of $C_{40}H_{18}^{2-}$.

Calculations of the model $[Cs^+]_2[C_{40}H_{18}^{2-}]$ complex also showed a similar shift of the naked $Cs^+$ ions toward the tether. However, it is less pronounced than that observed experimentally in **2** ($Cs\cdots C_5$ centroid 2.979 vs 3.474 Å, Table S2), indicating possible involvement of 18-crown-6 ether. The effect of crown ethers on the geometry of products has been seen before. For example, intermolecular interactions between the crown moieties and coronene monoanions were recently found responsible for an aligned solid-state packing and new coordination mode of the radical-anion of coronene.[18]

For the next step, calculations of a larger system, $[Cs^+(18\text{-crown-}6)]_2[C_{40}H_{18}^{2-}]$, have been carried out. The expanded model was found to be in better agreement with the experimental structure, as both show a close shift in cesium binding toward the tether (distance from the hub is 3.574 Å (calc) vs 3.474 Å (exp)). The calculated intermolecular C−H$\cdots\pi$ contacts between the $[Cs^+(18\text{-crown-}6)]$ moieties and the charged bicorannulenyl are in the range 2.918−3.1741 Å. Thus, the exact positioning of the $Cs^+$ cation inside the bowl is determined by the interplay of the electrostatic forces with the dianionic bicorannulenyl core and the above intermolecular interactions.

For comparison, we have also modeled the Li-based SSIP system **1**. Geometrical parameters obtained for this model are in reasonable agreement with the experimental values (Table 1). As in the structure of **2**, the shift of $[Li^+(THF)_4]$ ions toward the dianion tether was observed. Since the isolated molecule was considered in calculations, such a shift cannot be attributed to the influence of crystal packing. It supports the previous conclusion about localization of the negative charge


dx.doi.org/10.1021/om500396m | Organometallics 2014, 33, 2874−2878

on the central carbon−carbon bond and its influence on the positioning of alkali metal counterions. Interestingly, the impact of positively charged ions on the electronic structure of the dianionic bicorannulenyl core was found most pronounced in the case of **2**. Polarization of the hydrocarbon core in **2** can be illustrated by atomic charges located on the symmetrically unique tether C atom and closely lying hub atoms of the g-bond (−0.11, −0.23, and −0.12 in **2** vs −0.09, −0.01, and −0.11 in free $[C_{40}H_{18}^{2-}]$, respectively) and is graphically evidenced from the MEP distribution (Figure 4). At the same

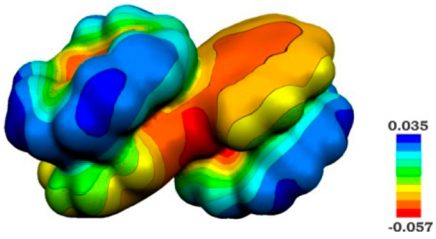


**Figure 4.** Molecular electrostatic potential map of $[Cs^+(18\text{-crown-}6)]_2[C_{40}H_{18}^{2-}]$.

time, the nature of bonding between two bowls remains essentially the same in all computed systems. In addition to the standard single $\sigma$-bond, it contains a substantial $\pi$-contribution. In terms of NBO analysis the first part is described as the result of coupling of two hybrid $sp^{1.75}$-orbitals with occupancy of the corresponding bonding NBO of ∼1.97*e*, whereas the $\pi$-contribution comes from interaction of two pure p-orbitals of aimed carbon atoms with the NBO occupancy of ∼1.75*e*. Importantly, the corresponding $\pi^*$-orbital has an occupancy equal to ∼0.45*e*, while the occupancy of $\sigma^*$ NBO was found to be ∼0.02*e* (see graphical representation of all NBO in Figure S9). These findings suggest the description of the tether bond as $\sigma$-type with a substantial $\pi$-component rather than a classical double bond. This description applies to all calculated systems, ranging from free $[C_{40}H_{18}^{2-}]$ to $[Cs^+]_2[C_{40}H_{18}^{2-}]$, $[Cs^+(18\text{-crown-}6)]_2[C_{40}H_{18}^{2-}]$, and $[Li^+(THF)_4]_2[C_{40}H_{18}^{2-}]$.

In conclusion, the first X-ray structural characterization of bicorannulenyl dianion has been accomplished for two alkali metal salts, revealing two different binding modes, namely, the "naked" form in the solvent-separated ion pair with small lithium ions vs unique double-concave metal coordination in the cesium product. In both cases, the central carbon−carbon bond between the corannulene units is shortened in comparison with neutral bicorannulenyl, as confirmed by X-ray crystallographic investigation. Notably, only the achiral $PM_{180}$ isomer is found in the solid-state products. Theoretical analysis of these systems revealed that polarization of the dianionic bicorannulenyl core is more pronounced in the case of $[Cs^+(18\text{-crown-}6)]_2[C_{40}H_{18}^{2-}]$, while the nature of bonding between two bowls remains essentially the same through the series.

## EXPERIMENTAL SECTION

**Preparation of $[Li^+(THF)_4]_2[C_{40}H_{18}^{2-}]$ (1).** THF (2 mL) was added to a flask containing Li (0.14 mg, 0.02 mmol, 2.5 equiv) and bicorannulenyl (4.00 mg, 0.008 mmol). The mixture was stirred for 6 h at room temperature and then filtered to afford a purple solution, which was layered with hexanes (2 mL) and kept at 10 °C. Dark purple blocks were collected in 70 h. They were washed several times with hexanes and dried. Yield: 5.2 mg, 60%. UV−vis (THF, nm): $\lambda_{max}$ 931. $^7$Li NMR (155.5 MHz, THF-$d_8$, −60 °C, ppm): $\delta$ 2.02. $^1$H NMR (400 MHz, THF-$d_8$, −80 °C, ppm): $\delta$ 4.33 (2H), 5.41 (2H), 5.53 (2H), 5.82 (2H), 5.93 (2H), 6.39 (2H), 6.64 (2H), 6.76 (2H), 7.46 (2H).

**Preparation of $[Cs^+(18\text{-crown-}6)]_2[C_{40}H_{18}^{2-}]$ (2).** THF (5 mL) was added to a flask containing bicorannulenyl (4.00 mg, 0.008 mmol) and 18-crown-6 (4.41 mg, 0.017 mmol, 2.1 equiv). The mixture was sonicated and stirred for ca. 2 h to produce a pale yellow solution. Cesium (2.24 mg, 0.017 mmol, 2.1 equiv) was added to the solution, and stirring was continued for another 2 h. The resulting purple mixture was filtered; the filtrate was layered with hexanes (5 mL) and kept at 10 °C. Dark purple plates were collected in 70 h. They were washed several times with hexanes and dried *in vacuo*. Yield: 6.7 mg, 65%. UV−vis (THF, nm): $\lambda_{max}$ 935. $^1$H NMR (400 MHz, THF-$d_8$, −80 °C, ppm): major isomer $\delta$ 4.37 (2H), 5.01(18-crown-6), 5.48 (2H), 5.64 (2H), 5.82 (2H), 5.96 (2H), 6.42 (2H), 6.66 (2H), 6.80 (2H), 7.46 (2H); minor isomer (poor solubility in THF) $\delta$ 2.55, 4.74, 6.09, 7.01, 7.17, 7.29, 7.63, 8.49.

## ASSOCIATED CONTENT

### Supporting Information

UV−vis and NMR spectra and X-ray structural details for **1** and **2**. This material is available free of charge via the Internet at http://pubs.acs.org. CCDC 991234 and 991235 contain the supplementary crystallographic data for **1** and **2**. These data can be obtained free of charge from the Cambridge Crystallographic Data Centre via www.ccdc.cam.ac.uk/data_request/cif.

## AUTHOR INFORMATION

### Corresponding Author

*E-mail: mpetrukhina@albany.edu. Fax: +1 518 442 3462. Phone: +1 518 442 4406.

### Notes

The authors declare no competing financial interest.

## ACKNOWLEDGMENTS

Financial support of this work from the National Science Foundation (CHE-1212441 and CHE-1337594, M.A.P.) and from Illinois Institute of Technology (start-up funds, A.Yu.R.) is gratefully acknowledged. S.N.S. also thanks the International Centre for Diffraction Data (ICDD) for the 2012 and 2013 Ludo Frevel Crystallography Scholarships.

## REFERENCES

(1) (a) Eisenberg, D.; Quimby, J. M.; Ho, D.; Lavi, R.; Besisvy, L.; Scott, L. T.; Shenhar, R. *Eur. J. Org. Chem.* **2012**, 6321−6327. (b) Furrer, F.; Linden, A.; Stuparu, M. C. *Chem.—Eur. J.* **2013**, *19*, 13199−13206. (c) Kawasumi, K.; Zheng, Q.; Segawa, Y.; Scott, L. T.; Itami, K. *Nat. Chem.* **2013**, *5*, 739−744.

(2) Eisenberg, D.; Quimby, J. M.; Scott, L. T.; Shenhar, R. *J. Phys. Org. Chem.* **2013**, *26*, 124−130.

(3) (a) Mehta, G.; Panda, G. *Tetrahedron Lett.* **1997**, *38*, 2145−2148. (b) Scott, L. T.; Cheng, P.-C.; Hashemi, M.; Bratcher, M. S.; Meyer, D. T.; Warren, H. B. *J. Am. Chem. Soc.* **1997**, *119*, 10963−10968. (c) Sygula, A.; Xu, G.; Marcinow, Z.; Rabideau, P. W. *Tetrahedron* **2001**, *57*, 3637−3644. (d) Butterfield, A. M.; Gilomen, B.; Siegel, J. S. *Org. Process Res. Dev.* **2012**, *16*, 664−676.

(4) (a) Sygula, A.; Fronczek, F. R.; Sygula, R.; Rabideau, P. W.; Olmstead, M. M. *J. Am. Chem. Soc.* **2007**, *129*, 3842−3843. (b) Kobryn, L.; Henry, W. P.; Fronczek, F. R.; Sygula, R.; Sygula, A. *Tetrahedron Lett.* **2009**, *50*, 7124−7127. (c) Yanney, M.; Sygula, A. *Tetrahedron Lett.* **2013**, *54*, 2604−2607.

(5) Bando, Y.; Sakurai, T.; Seki, S.; Maeda, H. *Chem.—Asian J.* **2013**, *8*, 2088−2095.

(6) (a) Topolinski, B.; Schmidt, B. M.; Kathan, M.; Troyanov, S. I.; Lentz, D. *Chem. Commun.* **2012**, *48*, 6298−6300. (b) Topolinki, B.;

Schmidt, B. M.; Higashibayashi, S.; Hidehiro, S.; Lentz, D. *Dalton Trans.* **2013**, *42*, 13809−13812.
(7) Eisenberg, D.; Filatov, A. S.; Jackson, E. A.; Petrukhina, M. A.; Scott, L. T.; Shenhar, R. *J. Org. Chem.* **2008**, *73*, 6073−6078.
(8) Amaya, T.; Kobayashi, K.; Hirao, T. *Asian J. Org. Chem.* **2013**, *2*, 642−645.
(9) (a) Ayalon, A.; Sygula, A.; Cheng, P.-C.; Rabinovitz, M.; Rabideau, P.; Scott, L. T. *Science* **1994**, *265*, 1065−1067. (b) Baumgarten, M.; Gherghel, L.; Wagner, M.; Weitz, A.; Rabinovitz, M.; Cheng, P.-C.; Scott, L. T. *J. Am. Chem. Soc.* **1995**, *117*, 6254−6257. (c) Aprahamian, I.; Hoffman, R. E.; Sheradsky, T.; Preda, D. V.; Bancu, M.; Scott, L. T.; Rabinovitz, M. *Angew. Chem., Int. Ed.* **2002**, *41*, 1712−1715. (d) Zabula, A. V.; Filatov, A. S.; Spisak, S. N.; Rogachev, A. Yu.; Petrukhina, M. A. *Science* **2011**, *333*, 1008−1011.
(10) Zabula, A. V.; Sevryugina, Y. V.; Spisak, S. N.; Kobryn, L.; Sygula, R.; Sygula, A.; Petrukhina, M. A. *Chem. Commun.* **2014**, *50*, 2557−2659.
(11) (a) Eisenberg, D.; Jackson, E. A.; Quimby, J. M.; Scott, L. T.; Shenhar, R. *Angew. Chem., Int. Ed.* **2010**, *49*, 7538−7542. (b) Eisenberg, D.; Quimby, J. M.; Jackson, E. A.; Scott, L. T.; Shenhar, R. *Chem. Commun.* **2010**, *46*, 9010−9012.
(12) Spisak, S. N.; Zabula, A. V.; Ferguson, M. V.; Filatov, A. S.; Petrukhina, M. A. *Organometallics* **2013**, *32*, 538−543.
(13) Spisak, S. N.; Zabula, A. V.; Filatov, A. S.; Rogachev, A Yu.; Petrukhina, M. A. *Angew. Chem., Int. Ed.* **2011**, *50*, 8090−8094.
(14) (a) Petrukhina, M. A.; Andreini, K. W.; Tsefrikas, V. M.; Scott, L. T. *Organometallics* **2005**, *24*, 1394−1397. (b) Filatov, A. S.; Rogachev, A. Yu.; Jackson, E. A.; Scott, L. T.; Petrukhina, M. A. *Organometallics* **2010**, *29*, 1231−1237. (c) Klett, J. *Chem. Commun.* DOI: 10.1039/c4cc01428f.
(15) (a) Amaya, T.; Sakane, H.; Hirao, T. *Angew. Chem., Int. Ed.* **2007**, *46*, 8376−8379. (b) Petrukhina, M. A. *Angew. Chem., Int. Ed.* **2008**, *47*, 1550−1552. (c) Amaya, T.; Wang, W.-Z.; Sakane, H.; Moriuchi, T.; Hirao, T. *Angew. Chem., Int. Ed.* **2010**, *49*, 403−406.
(16) Filatov, A. S.; Sumner, N. J.; Spisak, S. N.; Zabula, A. V.; Rogachev, A. Yu.; Petrukhina, M. A. *Chem.—Eur. J.* **2012**, *18*, 15753−15760.
(17) (a) Filatov, A. S.; Jackson, E. A.; Scott, L. T.; Petrukhina, M. A. *Angew. Chem., Int. Ed.* **2009**, *48*, 8473−8476. (b) Rogachev, A. Yu.; Filatov, A. S.; Zabula, A. V.; Petrukhina, M. A. *Phys. Chem. Chem. Phys.* **2012**, *14*, 3554−3567.
(18) Spisak, S. N.; Sumner, N. J.; Zabula, A. V.; Filatov, A. S.; Rogachev, A. Yu.; Petrukhina, M. A. *Organometallics* **2013**, *32*, 3773−3779.